Tracking river's pulse from space: A global analysis of river stage fluctuations

Yanan Zhao[1,2], Liguang Jiang[1,2], Xingxing Zhang[3], Junguo Liu[4,1]

[1]School of Environmental Science and Engineering, Southern University of Science and Technology, Shenzhen, 518055, China

[2]Shenzhen Key Laboratory of Precision Measurement and Early Warning Technology for Urban Environmental Health Risks, School of Environmental Science and Engineering, Southern University of Science and Technology, Shenzhen, 518055, China

[3]Institute of Geographic Sciences and Natural Resources Research, Chinese Academy of Sciences, Beijing, 100101, China

[4]Henan Provincial Key Laboratory of Hydrosphere and Watershed Water Security, North China University of Water Resources and Electric Power, Zhengzhou, 450046, China

Corresponding author: Liguang Jiang (jianglg@sustech.edu.cn)

Key Points:

Stage fluctuations of large rivers were estimated globally for the first time using satellite radar altimetry

Rivers in semi-arid regions have larger fluctuations than those in other climate regions

The top five river basins with the highest stage fluctuations (> 7 m) are the Orinoco, Mississippi, Yangtze, Irrawaddy, and Amazon basins

DOI: 10.1029/2023GL106399

Abstract

River stage fluctuation (RSF) is one of the most important factors influencing the physical, chemical, and ecological aspects of rivers. Despite widespread interest in river stage variations, there is currently no global benchmark of RSF and their spatial patterns. Our understanding of these characteristics remains limited. We used Sentinel-3 altimetry data to establish a benchmark dataset for RSF in wide rivers (width > 1 km). We conducted an initial investigation of the spatial patterns and inter-annual variability associated with RSF. The results show a wide range of fluctuation amplitudes spanning from a mere 1 m to 18 m. Notably, rivers in semi-arid regions exhibit more pronounced fluctuations. Further analyses indicate that human activities play a significant role in RSF. The results are of substantial interest to the scientific community, as they are closely linked to critical hydrological processes, including floods, river-floodplain dynamics, river-groundwater interaction, greenhouse gas emissions, and river restoration.

Plain Language Summary

Rivers show a seasonal rhythm over time due to multiple processes. A critical aspect of the rhythm is the river stage, which resembles the pulse of a river as it rises and falls. Traditionally, river stages have been monitored using gauging stations. However, these local monitoring networks fall short in providing a comprehensive global perspective on river stage fluctuations, which are directly linked to significant events like floods and droughts. Advanced Earth Observation techniques now offer a means to better understand the pulse of rivers on broader scales. Specifically, satellite radar altimetry serves as a valuable tool for river stage records by measuring water surface elevation, thereby providing insights into the normality or abnormality of river conditions. This study represents one of the first global-scale investigations into the patterns of river stage fluctuations and inter-annual variability spanning from 2016 to 2022. Moreover, this new dataset holds practical value for related studies, such as the validation of the average depth of the channel when the river is full, the assessment of river channel storage variation, the facilitation of river navigation, stepwise ecological restoration, and more.

1 Introduction

Rivers are complex ecosystems which have formed over a long time and continue to evolve (Humphries et al., 2014). The interactions between rivers and their landscapes work in different dimensions. Longitudinally, rivers flow down the river channel while laterally moving onto floodplains, and vertically, interact with groundwater (Hadeed & Thomson, 2006; Poff, 2019). However, human activities can accelerate and redirect the evolution of such ecosystems (Hadeed & Thomson, 2006). With the advance of urbanization and economic development, rivers and their watersheds have been utilized heavily, leaving very few systems in a natural state, or freely flowing. For instance, the flow regime of the Lancang River has been changed due to the regulation as well as climate change (Liu et al., 2022; Zhang et al., 2023). Munoz et al. (2018) revealed that river engineering largely contributes to the increased flood magnitudes. At the global scale, Grill et al. (2019) showed that only 37% of rivers longer than 1000 km remain free-flowing over their entire length and 23% flow uninterrupted to the ocean.

River level (stage), representing the vertical dimension of a river, is a key variable for a wide range of hydraulic, hydrological, ecological, biochemical, and geomorphological processes (Alsdorf et al., 2000; Koel & Sparks, 2002; Saleh et al., 2011). Beyond the wide applications of river stage for flood/drought assessment (Jiang, Zhao, et al., 2023; Zhong et al., 2022), hydrodynamic model calibration and validation (Jiang et al., 2021; Schneider et al., 2018), discharge estimation (Leon et al., 2006; Zakharova et al., 2020), the variations in river stage are acknowledged to affect local groundwater flow because river stage fluctuations can influence hydraulic gradients between river and groundwater systems (Boutt & Fleming, 2009; Jasechko et al., 2021). During wet seasons, direct runoff to a river can increase the river stage and reverse the normal groundwater hydraulic gradient toward the river. Therefore, river water moves into the adjacent aquifer. During dry seasons, the river stage declines, and the normal hydraulic gradient is reestablished. Consequently, the stored water is discharged back into the river. This process is often termed "bank storage" (Squillace, 1996). In turn, the exchange of water flow can affect the water temperature and chemistry (Gu et al., 2012). Stage fluctuations can thus facilitate the movement of water and solutes between rivers and adjoining hyporheic and riparian zones and aquifers, influencing biochemical and ecological cycles (Baratelli et al., 2016; Ferencz et al., 2019). Similarly, river stage fluctuation plays an important role in the river-floodplain systems (Bates et al., 2000). For instance, river stages basically determine the connectivity between rivers and floodplains, which supports a range of ecosystem functions. Moreover, river stage fluctuations play an important role in shaping river geomorphology, such as the river bank erosion (Liang et al., 2015) and also riverine methane emissions (Raymond et al., 2012; Rocher-Ros et al., 2023).

Monitoring river stage and its fluctuations is of utmost importance. It serves various crucial purposes such as characterizing the patterns and processes of a river system, estimating river storage dynamics, managing hydrological disasters, validating hydraulic/hydrodynamic models, and enhancing our understanding of many interconnected hydro-biogeochemical processes (Humphries et al., 2014). Recent studies (e.g., Coss et al., 2023; Trautmann et al., 2023) have highlighted the importance of river storage to the total water storage dynamics. However, the knowledge of stage fluctuations on a global scale is still very poor. One of the main obstacles impeding a global assessment of river stage fluctuations is due to the lack of *in-situ* monitoring networks (Ruhi et al., 2018). To the best of our knowledge, there is no global river stage network so far. The advent of Earth Observation from space has created new opportunities for better understanding river systems. The recently launched Surface Water and Ocean Topography mission (Biancamaria et al., 2016) might alleviate this problem in the near future. Currently, satellite altimetry has greatly increased the availability of water surface elevation (WSE) data globally (Abdalla et al., 2021; Birkett, 1995; Crétaux et al., 2015; Jiang et al., 2019, 2021). For example, Coss et al. (2020) produced a global river altimetry dataset covering the period from 2002 to 2016, which incorporated 932 virtual stations (VS) by leveraging data from the Envisat and Jason-2 missions. In contrast, a recent study by Jiang et al. (Jiang, Zhao, et al., 2023) revealed that Sentinel-3 constellation has created an impressive number of over 80,000 VSs, despite their assessment being based on more than 3,000 VSs. The spatial coverage is mainly affected by the altimeter orbits. Compared to the Jason series, the new generation radar altimetry mission, Sentinel-3, based on a constellation of two satellites, allows the spatial coverage much denser than previous missions of short repeat orbit. On top of its higher data quality as reported by previous studies (Gao et al., 2019; Halicki & Niedzielski, 2022; Jiang et al., 2020; Jiang, Nielsen, et al., 2023; Jiang, Zhao, et al., 2023; Kittel et al., 2021), its spatial coverage allows us to monitor and assess global river dynamics (Jiang, Nielsen, et al., 2023).

In this context, the main purpose of this study is to assess global river stage fluctuations for the first time. To achieve the objective, we first built a global river level dataset based on Sentinel-3 altimetry data. This dataset enabled us to compute river stage fluctuations based on the time series of river WSE. Subsequently, we conducted an analysis of long-term river stage fluctuations along with an assessment of the annual fluctuations' variability. Additionally, we explored the impact of human activities on these river stage fluctuations. The water level time series and stage fluctuations are made free and publicly accessible to the scientific community.

2 Data and Methods

2.1 Altimetry Data

Data quality of satellite altimetry has been greatly improved since the 1990s (Jiang, Nielsen, et al., 2023). Sentinel-3 mission, comprising a constellation of two satellites, Sentinel-3A (S3A) and Sentinel-3B (S3B), provides nearly global observations with a cycle period of 27 days (Donlon et al., 2012). Both satellites carry a Ku-band SAR altimeter operating in open-loop mode, providing more reliable and high-quality observations. Together, the distance between nominal ground tracks is about 52 km, allowing sample more river reaches. In this study, level-2 GRD Land products at Non Time Critical (NTC) timeliness were collected for the periods of 2016-2022 and 2018-2022, respectively, for S3A and S3B.

2.2 Data Processing

Water surface elevation (WSE) for each 20 Hz measurement is calculated according to the equation below,

$$WSE = h - (R_{unc} + R_{geo}) - N,$$

where, h is the altitude of satellite, R_{unc} is the retracked range without geophysical and atmospheric corrections, R_{geo} is the sum of atmospheric (ionospheric delay, dry and wet tropospheric delays) corrections and geophysical (pole tides, solid earth tides) corrections, and N is the EGM2008 geoid height. Note that we used the default OCOG retracked R_{unc} for most VSs. However, this retracker cannot deliver useful R_{unc} over the Yangtze river due to heavily contaminated waveforms as reported by our previous study (Jiang et al., 2020). Therefore, we used MWaPP+ retracker (Jiang et al., 2020) to obtain the retracked R_{unc}.

To calculate the river stage fluctuation, time series of WSE at Virtual stations (VS) are needed. VS were first created by intersecting the nominal sentinel-3 ground tracks with river centerlines from the Global River Widths from Landsat database (Allen & Pavelsky, 2018a). Since this study is conducted at the global scale, we focused on VS where the river is wider than 1 km.

WSE observations were filtered following three steps. Firstly, we used water occurrence (< 20%) (indicating the likelihood one observation is on water, (Pekel et al., 2016)) and DEM (the difference between the DEM value and observation, i.e., $\Delta H > 30$ m) to remove spurious observations. Secondly, we used the median of absolute deviation (MAD) to filter out the outliers for each pass. Thirdly, we applied IQR and support vector regression (SVR) to observations of all passes to obtain final reliable observations. Then we finally used the tsHydro tool (Nielsen et al., 2015) to obtain the WSE for each pass. In cases where tsHydro fails, we instead used the median value of each track to represent the WSE.

To ensure accuracy of WSE retrievals and remove any outliers that were not filtered by the automatic methods, we also manually checked those with extremely large/small fluctuations. Therefore, the quality of WSE is slightly better than a previous study (Jiang, Zhao, et al., 2023), which is indicated by the lower median standard deviation of the along-track measurements, i.e., 11.19 cm and 11.22 cm for S3A and S3B, respectively. And the counterpart is 24.4 cm and 23.3 cm from (Jiang, Zhao, et al., 2023).

2.3 Stage Fluctuation Estimates and Analysis

In principle, the stage fluctuation is equal to the difference between the highest and lowest WSE within a given period. However, satellite altimetry observations are subject to uncertainty and spurious outliers. Therefore, instead of the maximum and minimum of WSE, the 95th and 5th percentiles were used. Nevertheless, we calculated stage fluctuation using both methods, and they yielded a high level of consistency (see Figure S1). Thus, the annual fluctuation and long-term fluctuation were estimated by the difference between the 95th and 5th percentiles of WSE observations within a calendar year and the whole study period, respectively.

The variability of annual fluctuations is quantified by the standard deviation (STD) of annual fluctuations. To compare the variability across different rivers, the coefficient of variation (CV, also called relative variability) is used to normalize the influence of absolute fluctuation on the STD. Specifically, CV is calculated by dividing the STD of the annual fluctuations by the average annual fluctuation. To analyze global patterns in stage fluctuations, we also spatially aggregated VSs across large river basins.

2.4 Ancillary Data

Global Aridity Index and Potential Evapotranspiration Database - Version 3 (R. J. Zomer et al., 2022) was used to analyze river stage fluctuations over different climate zones. Similarly, the Global Runoff Data Center (GRDC) Major River Basins were used to investigate the spatial patterns of stage fluctuations. To analyze the human influence on river stage fluctuations, we broadly grouped VS into two categories based on the river flowing status, i.e., free-flowing river reach or non-free-flowing reach (G. Grill et al., 2019). Specifically, we used the connectivity status index (CSI) to reflect the degree to which a river reach is altered by human activities.

3 Results and Discussion

3.1 Long-term River Stage Fluctuation

Overall, river stage fluctuations of 3,272 VSs were estimated, among which 1,649 VSs are from S3A and 1,623 from S3B, respectively. Geographically, these VSs are mainly from the northern high latitude and the Equator. Their distributions along latitude and longitude of both S3A and S3B are generally the same (Figure 1), indicating a high level of consistency of the fluctuation estimates although the temporal coverage is slightly different. It should be noted that the temporal coverage matters since the river stage at 95^{th} and 5^{th} percentiles may be different and thus the fluctuation differs. Broadly, higher fluctuation amplitudes occur in South America, Siberia, and Asia. Moreover, the fluctuation amplitude increases gradually in the downstream direction, especially at the relatively less regulated Arctic rivers, Amazon, and Congo rivers, although discontinuities also appear at a few locations.

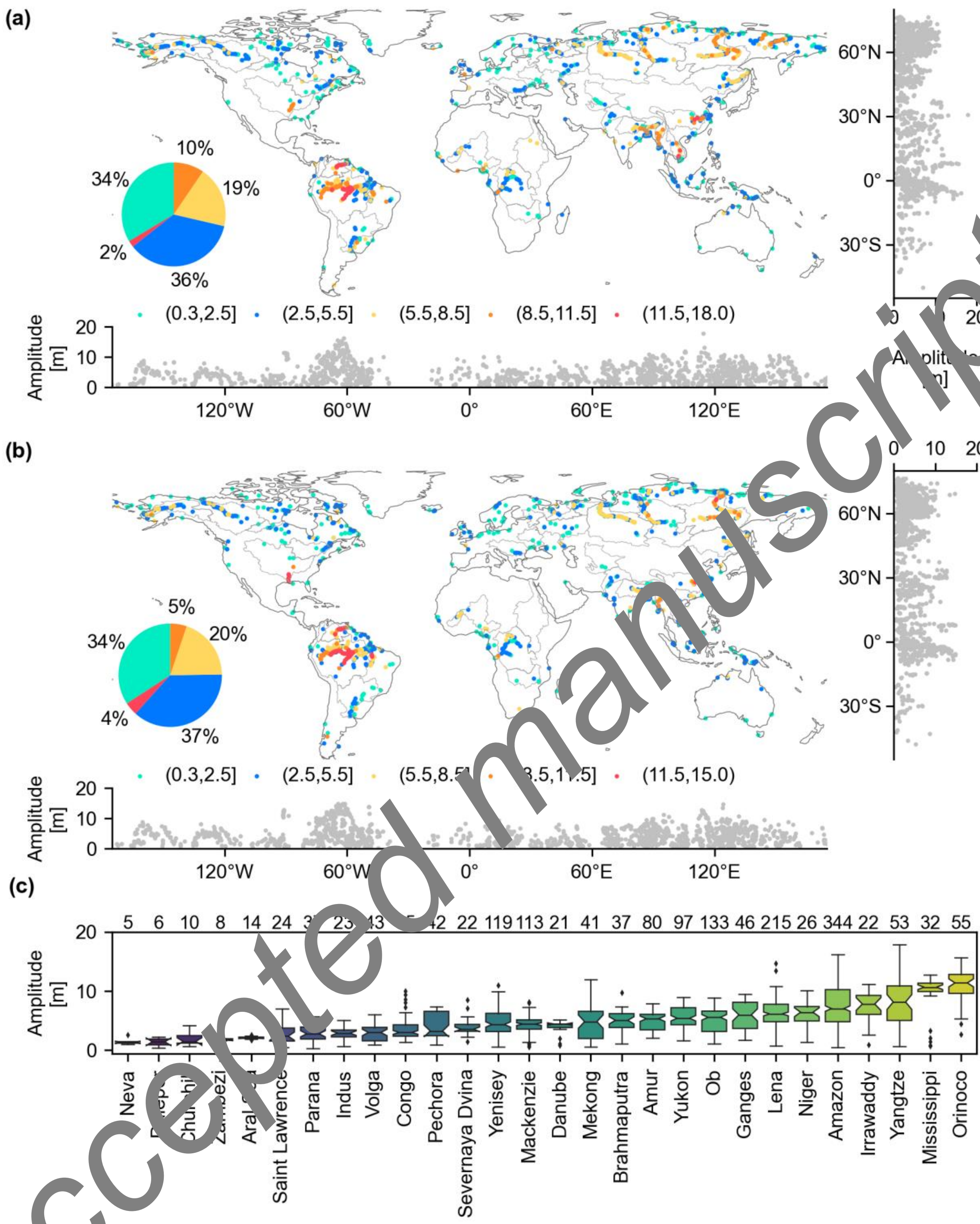

Figure 1. Distribution and statistics of river stage fluctuations on a global scale (a: Sentinel-3A; b: Sentinel-3B), and (c) fluctuation statistics at basin scales including data from both satellites. Only basins with at least 5 VSs (numbers are given on the top) are included. The pie chart in (a) and (b) shows the percentage of the five fluctuation classes, the colors of which are associated with that of the pie chart.

Global statistics show that the median fluctuation amplitude of S3A is about 3.63 m, ranging from 0.38 to 17.84 m, while that of S3B are 3.55 m and 0.30 ~ 14.89 m. The smaller fluctuations are mainly from VSs located at the most downstream reaches running into seas, where the stage peaks are attenuated. This is supported by the relationships between fluctuation variability and the distance to the outlet (Figures S2, S3 & S4). As shown in Figure 1, over two thirds (70% and 71% for S3A and S3B) of VSs exhibit stage fluctuation below 5.5 m, whereas a smaller proportion (2% and 4% for S3A and S3B) with a fluctuation amplitude over 11.5 m. These hot spots (clusters of larger fluctuations) clearly spread over the Orinoco, Madeira, Solimões, lower Mekong, and Yangtze rivers. Specifically, the middle reach of the third largest river, Orinoco, shows a mean fluctuation of 11.94 m. The Madeira, although regulated by reservoirs, has a much larger mean fluctuation of 12.63 m. The reach of Solimões between Iquitos and Manaus shows a mean fluctuation of 10.46 m. While over the Mekong and Yangtze, just a few VSs exceed the threshold of 11.5 m (Figures 1a &1b).

In terms of river basins, the 28 mega river basins exhibit contrasting stage fluctuation patterns (Figure 1c). Notably, the Orinoco, Mississippi, Yangtze, Irrawaddy, and Amazon basins emerge as the top five with the highest median amplitudes, that is, 11.38 m, 10.65 m, 8.14 m, 7.80 m, and 7.02 m, respectively. However, the interquartile ranges (middle 50%) and whiskers (outside the middle 50%) of Amazon and Yangtze are larger than that of other rivers due to their complex river networks, highlighting the pronounced spatial variability of river stage fluctuations across the whole basins. Besides, five Arctic rivers, i.e., Lena, Ob, Yukon, Mackenzie, and Yenisey also exhibit large fluctuations.

To understand the fluctuation in regard to climate aridity, VSs were grouped into five categories (hyper arid, arid, semi-arid, dry sub-humid, and humid). As shown in Figure 2, the general patterns are very similar for both altimeters. It should be noted that the temporal coverage of S3A is longer than that of S3B, thus the fluctuation amplitude is slightly different. As expected, the humid regions have the largest number of VSs, accounting for 68.0% and 71.5% of VSs for S3A and S3B, respectively. Regarding the fluctuation amplitude, the semi-arid regions exhibit the greatest median fluctuation amplitude, i.e., 4.60 m and 4.35 m for S3A and S3B. The median amplitude in both the dry sub-humid and humid regions are smaller, with values of 3.61 m and 3.4[illegible] m, and 3.56 m and 3.40 m for S3A and S3B, respectively (see boxplots in Figure 2). In contrast, the arid regions possess less (ca. 2%) large rivers, and these rivers have relatively smaller stage fluctuations in the order of 2.5 m. As shown in Figure 2, the relationship between stage fluctuation and aridity is parabolic instead of monotonic in general. This pattern is likely dominated by the seasonality of precipitation and evapotranspiration (Feng et al., 2019), but may also be affected by the interactions between surface water and groundwater. In drier climates, rivers are more common to lose water to recharge surrounding aquifers (Jasechko et al., 2021). This may explain the observed larger fluctuations in semi-arid than in humid climate.

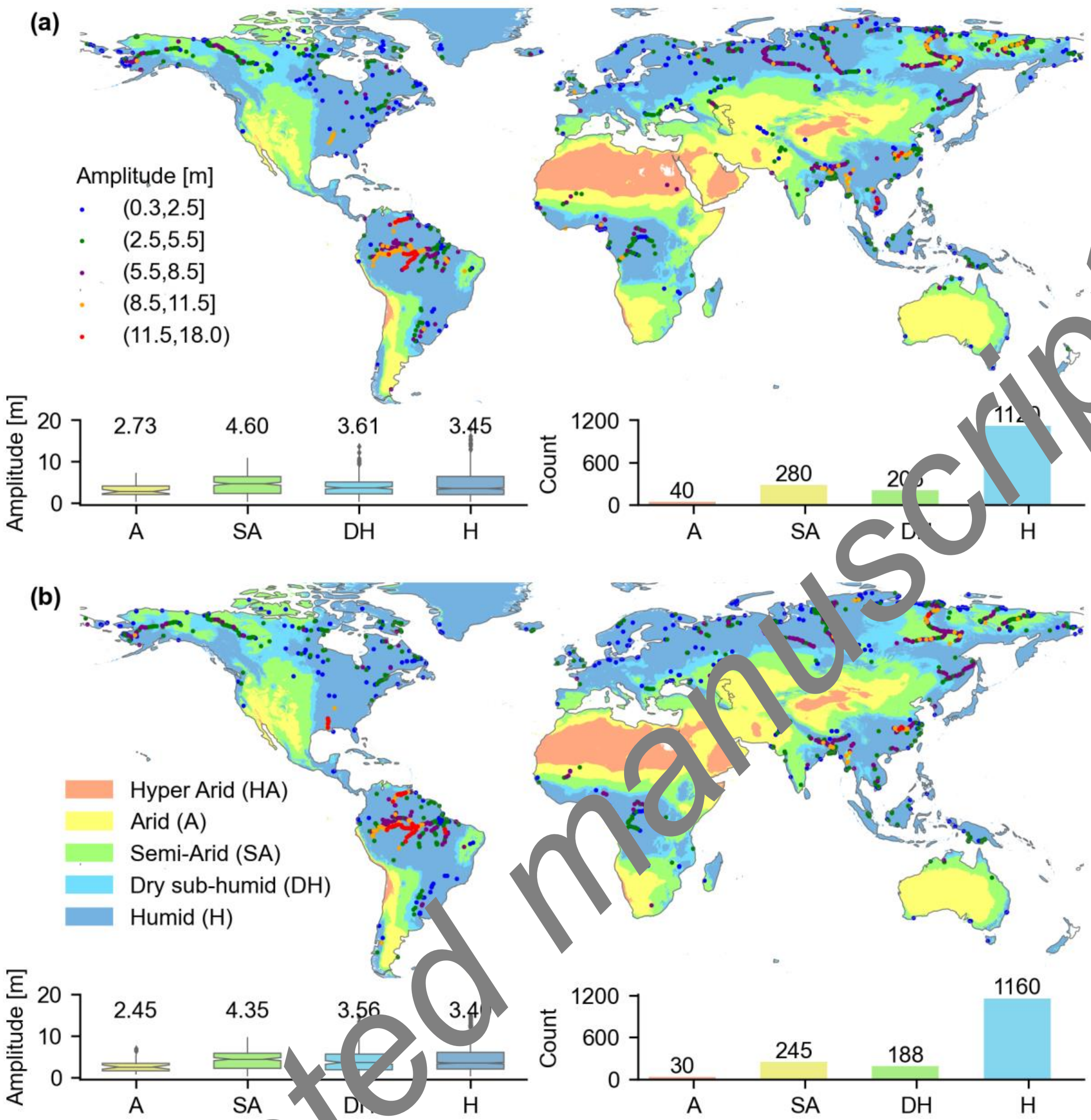

Figure 2. Global patterns (a: Sentinel-3A; b: Sentinel-3B) of river stage fluctuation in regard to climate aridity. Climate classification scheme (hyper arid, arid, semi-arid, dry sub-humid, and humid) is based on the global aridity index. Note that due to very few VSs located in hyper arid region, these VSs (3 from S3A) are not included in this figure.

3.2 Variability in Annual Stage Fluctuation

Since we calculated annual stage fluctuation using calendar year, the results shown are based on VSs with data spanning from 2017 to 2022 (S3A). Here we did not use S3B due to the short period (i.e., four years). The coefficient of variation (CV) provides a measure of temporal variability relative to the mean. Overall, the year-to-year variability in annual fluctuations is within about 35% of the mean. As indicated by the pie chart (Figure 3a), over 85% of VSs have a relatively narrow range between 0.02 and 0.35 over a broad range of fluctuation amplitudes (i.e., 0.27 - 14.69 m). Details of the mean and standard deviation of fluctuation amplitudes refer to Figure S5. Smaller CV values are mainly clustered in the tropical regions, while larger CV values (> 0.35) can be seen in the high latitude rivers (Figure 4a). At basin scales, CV ranges from 0.11 to 0.37, with the largest ones found in the Neva, Parana, Mackenzie, Dnieper, and Pechora River basins, while the smallest ones in Brahmaputra, Orinoco, Aral Sea, Indus, and Niger river basins (Table S1).

In the boxplots depicted in Figure 3b, there are observable maximum and minimum fluctuations at the VSs on a global scale each year. Nonetheless, these fluctuations vary from one year to another. Specifically, about 23.2% of VSs have maximum fluctuations in 2022 while only 11.9% in 2019, which may indicate a larger variation in water balance within 2022. In contrast, over 23.9% of VSs experienced the minimum fluctuation in 2019 while only 9.7% in 2020. This may be explained by the low variability in water balance in 2019. However, the results have to be carefully interpreted since a smaller fluctuation does not necessarily imply a drought. At basin scales, we can clearly see that arctic river basins (e.g., Lena, Mackenzie, Ob, Yenisey, Yukon) experienced larger fluctuations in the last 3 years (in warm colors in Figure 3c) while the south-hemisphere river basins (e.g., Orinoco, Congo, Parana, Niger, Zambezi) mainly in 2018 and 2019 (in cold colors Figure 3c). For example, in 2022, 29.2% of VSs in the Lena River basin and 35.1 of VSs in the Mackenzie River basin experienced the largest fluctuations. In contrast, in 2020, 60.0% of VSs in the Yukon River basin showed significant variances. The Arctic experienced notable precipitation in recent years, especially in the 2021/22 water year (Walsh et al., 2023), which might relate to the variability in large-scale atmospheric and oceanic circulations, especially the North Atlantic Oscillation and Arctic Oscillation (Bintanja et al., 2020; Haine et al., 2015; Peterson et al., 2002). Moving back in time, 44.2% of VSs in the Congo and 35.3% of VSs in the Parana exhibited the most pronounced fluctuations in 2019. The Indian Ocean Dipole might be responsible for the excess precipitation over Congo Basin while El Niño-Southern Oscillation is probably related to the drought in Parana Basin (Antico & Vuille, 2022; Jarugula & McPhaden, 2023). Furthermore, in 2018, the Orinoco and Niger basins saw their largest fluctuations at 81.3% and 50.0% of VSs respectively (Figure 3c and Table S2). The variability of these tropical rivers might be explained by the El Niño–Southern Oscillation events (Amarasekera et al., 1997). Further investigation is beyond the scope of this study.

Attribution of the observed variability is challenging. Aside from human activity, many factors affect the spatial patterns of the observed variability as shown in Figure 3a, such as climate, water availability, geomorphology of river channel, etc. Through the analysis of aridity and variability in stage fluctuation, a negative relationship is revealed. That is, the drier the climate, the larger the variability in stage fluctuation (i.e., the larger CV values). This explains the smaller CV in the tropic regions and larger values in high latitude rivers (Figure S6a). However, this relationship is not monotonic but parabolic with the peak occurring around semi-arid climate (Figure S7). Additional analysis of variability in water balance (Figure S6b) shows that stage fluctuation variability is positively correlated to the variability of water balance (i.e., P - ET) in most river basins, which might be expected a *priori* because of the correlation between river discharge and stage. However, one should note that the variability of water balance is not directly comparable to the variability in annual stage fluctuations since no downstream accumulation is considered. Moreover, the calculated water balance (P-ET) over the high latitude rivers might be unrealistic due to the snow accumulating/melting processes.

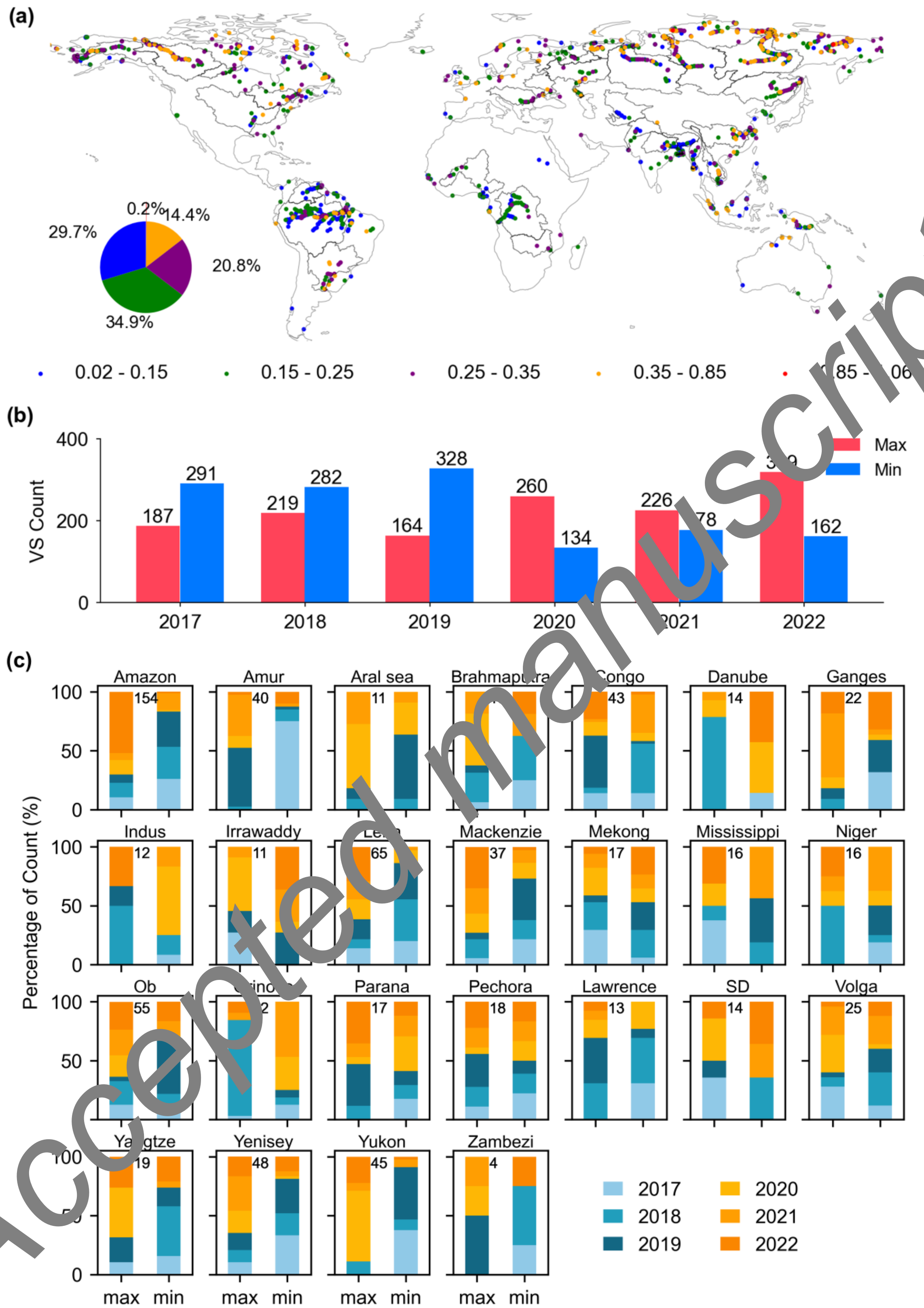

Figure 3. (a) Coefficient of variation (CV) of annual stage fluctuations (1,636 VSs); (b) the number of VSs for each year in which the maximum and minimum fluctuations occur. Here 1375 VSs with data covering the full 6 years were used. (c) similar to (b) but for 25 river basins. Note that basins with data less than 6 years were excluded.

3.3 River stage fluctuation affected by human activities

Besides climate effects, river stage changes behind dams can be very dramatic, highly unnatural. As shown in section 3.1, the largest fluctuations are found in big rivers, such as the Amazon, Orinoco, Madeira, Yangtze, etc. However, river fluctuations do not consistently exhibit high amplitude along the river, largely due to regulatory interventions. Besides, it is important to note that the size of a river, even in cases of closed river basins where water use surpasses the available renewable water supply, such as the Colorado (Molle et al., 2010) does not necessarily correlate with the amplitude of stage fluctuations. This phenomenon is primarily attributed to the influence of intensive human activities (Di Baldassarre et al., 2018). To assess the degree of human-induced alterations within a river reach, we used the river connectivity status index (CSI), given the absence of reservoir operation rules.

Here, we used the weighted linear regression to take the spread of fluctuation amplitude within a CSI bin into consideration. As shown in Figure 4, the fluctuation amplitude has a positively significant relationship with CSI (*p* value < 0.005). As the CSI increases, there is a tendency toward larger amplitude. In other words, as rivers flow more freely with few dams, the stage fluctuations are likely larger. Statistically, 51.2% of the variation in stage fluctuation amplitude can be explained by the CSI. This is somewhat reasonable considering the conditions followed (G. Grill et al., 2019). Firstly, the CSI mainly describes river connectivity that may be attributed to different factors instead of just reservoirs and dams. Depending on the capacity and main purpose of reservoirs, the impact on river stage fluctuations can be different and the relationship may be highly nonlinear. Secondly, these rivers intrinsically have different fluctuations even though we only considered those in humid regions. Therefore, the larger fluctuations with CSI of 40-45%, 45-50%, and 70-75% may be due to other factors. Nevertheless, river stage fluctuation is heavily affected by human activities as reflected by the linear correlation (Figure 4) and Spearman rank correlation (ρ > 0.61 and *p* value < 0.05). More effort is needed to delve into the quantitative identification of human impacts on river stage fluctuations.

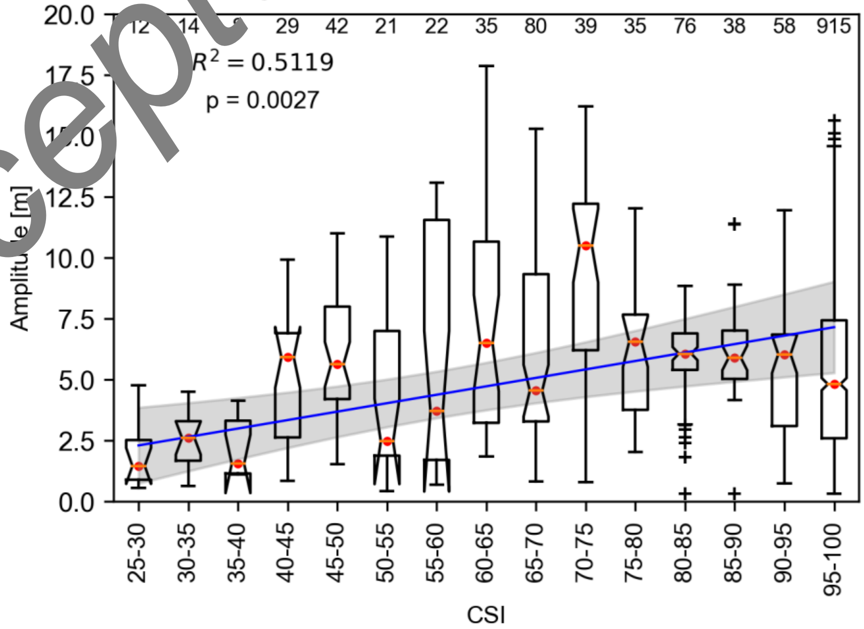

Figure 4. The relationship between river stage fluctuation amplitude and CSI (Connectivity Status Index) binned with a five percent interval using both S3A and S3B VSs over the Humid climate. The blue line shows the weighted linear regression, and the grey shaded area represents the 95% confidence interval. R^2 and p-values are in the upper left corner and the number of VSs in each bin is also labeled at the top of each box.

4 Conclusion and Perspectives

The high-quality Sentinel-3 altimetry observations, provided by a dual-satellite constellation, offer an excellent balance between spatial and temporal coverage for monitoring river dynamics. This study presents the first attempt to estimate stage fluctuations in major global rivers using satellite altimetry data. On a global scale, the median maximum river stage fluctuation is about 3.63 m during the period of 2016 and 2022, and median annual fluctuation is 2.88 m. At basin scales, the Orinoco, Mississippi, Yangtze, Irrawaddy, and Amazon basins stand out as the top five with the highest median amplitudes (> 7 m). Our results also show that the median fluctuation is larger over semi-arid climate regions than by sub-humid and humid regions. The observed fluctuation amplitudes have a significant correlation with river connectivity status index, indicating large impacts of human activities on river stage fluctuation.

The presented results are conservative and may be underestimated due to the relatively short period of time of Sentinel-3 data on one hand, which may not be long enough to represent the climatology of river stage fluctuations for certain rivers. On the other hand, the 27-day repeat cycle of Sentinel-3 may miss capturing extreme high peaks and low troughs. As the continuity of high-quality altimetric observations from Sentinel-3C and -3D, a more reliable climatology of river fluctuations can be established. Further, a longer record can reflect the changes due to, for example, the building of river dikes.

Despite the short period, this study presents a first global picture of large river stage fluctuations based on satellite observations of river water surface elevation. Thus, this study enhances our understanding of global river dynamics in the vertical dimension. We anticipate the stage fluctuation dataset will facilitate related work in a broad range of geosciences. For instance, river stage fluctuations can be used to estimate river channel storage changes (Coss et al., 2023). In analogy to the estimation of lake or reservoir storage change, channel storage change can be estimated by combining the stage fluctuation and corresponding river area derived from imagery for a given reach. In addition, the information about river stage fluctuation can guide river navigation (Trigg et al., 2022). Adequate water depth in the channel is required to allow ship transport safely through the river. This is especially pertaining to poorly gauged rivers.

Moreover, it can be used as an alternative bankfull depth for discharge estimation and hydrodynamic modeling (Andreadis et al., 2013; Mersel et al., 2013). We did a comparison with the bankfull depths from Andreadis et al. (2013) (hereafter referred to as Andreadis2013). Note that the Andreadis2013 bankfull depths were generated using a regression equation ($d = 0.27Q^{0.3}$) based on estimated mean annual peak flow. Nevertheless, we expect that our stage fluctuations should be always lower than the Andreadis2013 bankfull depths as we report actual change of river depth rather than the static maximum depth. Overall, we indeed see general agreements (Figure S8). About 67.2% of our fluctuations (based on the maximum and minimum) are within the Andreadis2013 confidence interval of bankfull depth, and the corresponding percentage is 54.3% if fluctuation calculation is based on the 95th and 5th percentiles. But still this comparison reveals inconsistencies. For instance, the observed fluctuations greatly exceed the Andreadis2013 bankfull depths (see Figure S8). This indicates the Andreadis2013 estimates are largely underestimated. This case contributes conservatively 10.3% of all considered locations based on the 95th and 5th percentiles, whereas it can be 19.0% using fluctuation calculated by the difference between the maximum and minimum. For this case, we strongly recommend adopting our fluctuations as alternatives to the values for bankfull depth. In principle, our fluctuations should be less representative over humid larger river basins, since these rivers seldom have very shallow river depths (i.e., unobservable depth is relatively larger). Last but not least, this dataset may also be useful to study the interactions between streamflow and groundwater (Jasechko et al., 2021).

Potentially, over 86,000 VSs can be established using S3A and S3B, while the number can still be very large (12,607) considering rivers wider than 300 m. Future work will expand the dataset through including more rivers of widths down to a few hundred meters. Since the large- to medium-sized rivers constitute a large proportion of global river networks, taking the pulse of these rivers is meaningful to better understand the spatial patterns and explore the regional differences. The findings hold significant interest for the scientific community as they are intimately connected to pivotal hydrological processes. These processes encompass a range of vital areas, including flood risk assessment, river-floodplain interactions, river-groundwater interplay, greenhouse gas emissions, and stepwise ecological restoration of rivers (Liu et al., 2021).

Acknowledgments

This work was partially supported by the Shenzhen Key Laboratory of Precision Measurement and Early Warning Technology for Urban Environmental Health Risks (ZDSYS20220606100604008), Shenzhen Science and Technology Program (KCXFZ20201221173601003), Henan Provincial Key Laboratory of Hydrosphere and Watershed Water Security, the CRSRI Open Research Program (Program SN: CKWV20221009/KY), and the SUSTech research start-up grants (Y01296129; Y01296229). The computation of this work was supported by the Center for Computational Science and Engineering at Southern University of Science and Technology.

Open Research

Data sets used in this study are all publicly available. Sentinel-3 altimetry data were downloaded from Copernicus Open Access Hub https://scihub.copernicus.eu/dhus/#/home (accessed 28 March 2023). Global River Widths from Landsat (GRWL) Database is from Allen & Pavelsky (2018a), available at Allen & Pavelsky (2018b). The river connectivity status index (CSI) data is from Grill et al. (2019), available at Grill & Lehner (2019). Arid index is from Zomer et al. (2022), available at Zomer & Trabucco (2022). The dataset produced in this study is available at (Zhao & Jiang, 2023).

References

Abdalla, S., Abdeh Kolahchi, A., Ablain, M., Adusumilli, S., Aich Bhowmick, S., Alou-Font, E., et al. (2021). Altimetry for the future: Building on 25 years of progress. *Advances in Space Research*, *68*(2), 319–363. https://doi.org/10.1016/j.asr.2021.01.022

Allen, G. H., & Pavelsky, T. M. (2018a). Global extent of rivers and streams. *Science*, *361*(6402), 585–588. https://doi.org/10.1126/science.aat0636

Allen, G. H., & Pavelsky, T. M. (2018b). Global River Widths from Landsat (GRWL) Database (V01.01) [Dataset]. Zenodo. https://doi.org/10.5281/zenodo.1297434

Alsdorf, D. E., Melack, J. M., Dunne, T., Mertes, L. A. K., Hess, L. L., & Smith, L. C. (2000). Interferometric radar measurements of water level changes on the Amazon flood plain. *Nature*, *404*(6774), 174–177. https://doi.org/10.1038/35004560

Amarasekera, K. N., Lee, R. F., Williams, E. R., & Eltahir, E. A. B. (1997). ENSO and the natural variability in the flow of tropical rivers. *Journal of Hydrology*, *200*(1–4), 24–39. https://doi.org/10.1016/S0022-1694(96)03340-9

Andreadis, K. M., Schumann, G. J.-P., & Pavelsky, T. (2013). A simple global river bankfull width and depth database. *Water Resources Research*, *49*(10), 7164–7168. https://doi.org/10.1002/wrcr.20440

Antico, A., & Vuille, M. (2022). ENSO and Paraná flow variability: Long-term changes in their connectivity. *International Journal of Climatology*, *42*(14), 7269–7279. https://doi.org/10.1002/joc.7643

Di Baldassarre, G., Wanders, N., AghaKouchak, A., Kuil, L., Rangecroft, S., Veldkamp, T. I. E., et al. (2018). Water shortages worsened by reservoir effects. *Nature Sustainability*, *1*(11), 617–622. https://doi.org/10.1038/s41893-018-0159-0

Baratelli, F., Flipo, N., & Moatar, F. (2016). Estimation of stream-aquifer exchanges at regional scale using a distributed model: Sensitivity to in-stream water level fluctuations, riverbed elevation and roughness. *Journal of Hydrology*, *542*, 686–703. https://doi.org/10.1016/j.jhydrol.2016.09.041

Bates, P. D., Stewart, M. D., Desitter, A., Anderson, M. G., Renaud, J.-P., & Smith, J. A. (2000). Numerical simulation of floodplain hydrology. *Water Resources Research*, *36*(9), 2517–2529. https://doi.org/10.1029/2000WR900102

Biancamaria, S., Lettenmaier, D. P., & Pavelsky, T. M. (2016). The SWOT Mission and Its Capabilities for Land Hydrology. *Surveys in Geophysics*, *37*(2), 307–337. https://doi.org/10.1007/s10712-015-9346-y

Bintanja, R., van der Wiel, K., van der Linden, E. C., Reusen, J., Bogerd, L., Krikken, F., & Selten, F. M. (2020). Strong future increases in Arctic precipitation variability linked to poleward moisture transport. *Science Advances*, *6*(7). https://doi.org/10.1126/sciadv.aax6869

Birkett, C. M. (1995). The contribution of TOPEX/POSEIDON to the global monitoring of climatically sensitive lakes. *Journal of Geophysical Research*, *100*(C12), 25179. https://doi.org/10.1029/95JC02125

Boutt, D. F., & Fleming, B. J. (2009). Implications of anthropogenic river stage fluctuations on mass transport in a valley fill aquifer. *Water Resources Research*, *45*(4). https://doi.org/10.1029/2007WR006526

Coss, S., Durand, M., Yi, Y., Jia, Y., Guo, Q., Tuozzolo, S., et al. (2020). Global River Radar Altimetry Time Series (GRRATS): new river elevation earth science data records for the hydrologic community. *Earth System Science Data*, *12*(1), 137–150. https://doi.org/10.5194/essd-12-137-2020

Coss, S., Durand, M. T., Shum, C. K., Yi, Y., Yang, X., Pavelsky, T., et al. (2023). Channel Water Storage Anomaly: A New Remotely Sensed Quantity for Global River Analysis. *Geophysical Research Letters*, *50*(1). https://doi.org/10.1029/2022GL100185

Crétaux, J., Biancamaria, S., Arsen, A., Bergé-nguyen, M., & Becker, M. (2015). Global surveys of reservoirs and lakes from satellites and regional application to the Syrdarya river basin. *Environmental Research Letters*, *10*(1), 15002. https://doi.org/10.1088/1748-9326/10/1/015002

Donlon, C., Berruti, B., Buongiorno, A., Ferreira, M. H., Féménias, P., Frerick, J., et al. (2012). The Global Monitoring for Environment and Security (GMES) Sentinel-3 mission. *Remote Sensing of Environment*, *120*(2012), 37–57. https://doi.org/10.1016/j.rse.2011.07.024

Feng, X., Thompson, S. E., Woods, R., & Porporato, A. (2019). Quantifying Asynchronicity of Precipitation and Potential Evapotranspiration in Mediterranean Climates. *Geophysical Research Letters*, *46*(24), 14692–14701. https://doi.org/10.1029/2019GL085653

Ferencz, S. B., Cardenas, M. B., & Neilson, B. T. (2019). Analysis of the Effects of Dam Release Properties and Ambient Groundwater Flow on Surface Water-Groundwater Exchange Over a 100-km-Long Reach. *Water Resources Research*, *55*(11), 8526–8546. https://doi.org/10.1029/2019WR025210

Gao, Q., Makhoul, E., Escorihuela, M. J., Zribi, M., Seguí, P. Q., García, P., & Roca, M. (2019). Analysis of retrackers' performances and water level retrieval over the Ebro River basin using sentinel-3. *Remote Sensing*. https://doi.org/10.3390/RS11060718

Grill, G., Lehner, B., Thieme, M., Geenen, B., Tickner, D., Antonelli, F., et al. (2019). Mapping the world's free-flowing rivers. *Nature*, *569*(7755), 215–221. https://doi.org/10.1038/s41586-019-1111-9

Grill, Günther, & Lehner, B. (2019). Mapping the world's free-flowing rivers: data set and technical documentation [Data set]. figshare. Retrieved from https://doi.org/10.6084/m9.figshare.7688801.v1

Gu, C., Anderson, W., & Maggi, F. (2012). Riparian biogeochemical hot moments induced by stream fluctuations. *Water Resources Research*, *48*(9), 2011WR011720. https://doi.org/10.1029/2011WR011720

Hadeed, L., & Thomson, B. (2006). Free-Flowing Rivers: Economic Luxury or Ecological Necessity? *WWF*, 1–41. Retrieved from http://wwf.panda.org/about_our_earth/about_freshwater/freshwater_news/?uNewsID=62020

Haine, T. W. N., Curry, B., Gerdes, R., Hansen, E., Karcher, M., Lee, C., et al. (2015). Arctic freshwater export: Status, mechanisms, and prospects. *Global and Planetary Change*, *125*, 13–35. https://doi.org/10.1016/j.gloplacha.2014.11.013

Halicki, M., & Niedzielski, T. (2022). The accuracy of the Sentinel-3A altimetry over Polish rivers. *Journal of Hydrology*, *606*, 127355. https://doi.org/10.1016/j.jhydrol.2021.127355

Humphries, P., Keckeis, H., & Finlayson, B. (2014). The River Wave Concept: Integrating River Ecosystem Models. *BioScience*, *64*(10), 870–882. https://doi.org/10.1093/biosci/biu130

Jarugula, S., & McPhaden, M. J. (2023). Indian Ocean Dipole affects eastern tropical Atlantic salinity through Congo River Basin hydrology. *Communications Earth & Environment*, *4*(1), 366. https://doi.org/10.1038/s43247-023-01027-6

Jasechko, S., Seybold, H., Perrone, D., Fan, Y., & Kirchner, J. W. (2021). Widespread potential loss of streamflow into underlying aquifers across the USA. *Nature*, *591*(7850), 391–395. https://doi.org/10.1038/s41586-021-03311-x

Jiang, L., Andersen, O. B., Nielsen, K., Zhang, G., & Bauer-Gottwein, P. (2019). Influence of local geoid variation on water surface elevation estimates derived from multi-mission altimetry for Lake Namco. *Remote Sensing of Environment*, *221*(November 2018), 65–79. https://doi.org/10.1016/j.rse.2018.11.004

Jiang, L., Nielsen, K., Dinardo, S., Andersen, O. B., & Bauer-Gottwein, P. (2020). Evaluation of Sentinel-3 SRAL SAR altimetry over Chinese rivers. *Remote Sensing of Environment*, *237*(October 2019), 111546. https://doi.org/10.1016/j.rse.2019.111546

Jiang, L., Westphal Christensen, S., & Bauer-Gottwein, P. (2021). Calibrating 1D hydrodynamic river models in the absence of cross-section geometry using satellite observations of water surface elevation and river width. *Hydrology and Earth System Sciences*, *25*(12), 6359–6379. https://doi.org/10.5194/hess-25-6359-2021

Jiang, L., Nielsen, K., & Andersen, O. B. (2023). Improvements in mountain lake monitoring from satellite altimetry over the past 30 years – lessons learned from Tibetan lakes. *Remote Sensing of Environment*, *295*(December 2022), 113702. https://doi.org/10.1016/j.rse.2023.113702

Jiang, L., Zhao, Y., Nielsen, K., Andersen, O. B., & Bauer-Gottwein, P. (2023). Near real-time altimetry for river monitoring—a global assessment of Sentinel-3. *Environmental Research Letters*, *18*(7), 074017. https://doi.org/10.1088/1748-9326/acdd16

Kittel, C. M. M., Jiang, L., Tøttrup, C., & Bauer-Gottwein, P. (2021). Sentinel-3 radar altimetry for river monitoring – a catchment-scale evaluation of satellite water surface elevation from Sentinel-3A and Sentinel-3B. *Hydrology and Earth System Sciences*, *25*(1), 333–357. https://doi.org/10.5194/hess-25-333-2021

Koel, T. M., & Sparks, R. E. (2002). Historical patterns of river stage and fish communities as criteria for operations of dams on the Illinois river. *River Research and Applications*, *18*(1), 3–19. https://doi.org/10.1002/rra.630

Leon, J. G., Calmant, S., Seyler, F., Bonnet, M.-P., Cauhopé, M., Frappart, F., et al. (2006). Rating curves and estimation of average water depth at the upper Negro River based on satellite altimeter data and modeled discharges. *Journal of Hydrology*, *328*(3–4), 481–496. https://doi.org/10.1016/j.jhydrol.2005.12.006

Liang, C., Jaksa, M. B., Ostendorf, B., & Kuo, Y. L. (2015). Influence of river level fluctuations and climate on riverbank stability. *Computers and Geotechnics*, *63*, 83–98. https://doi.org/10.1016/j.compgeo.2014.08.012

Liu, L., Cui, W., Tian, Z., & Jia, J. (2021). Theory of stepwise ecological restoration. *Chinese Science Bulletin*, *66*(9), 1014–1025. https://doi.org/10.1360/TB-2020-1128

Liu, J., Chen, D., Mao, G., Irannezhad, M., & Pokhrel, Y. (2022). Past and Future Changes in Climate and Water Resources in the Lancang–Mekong River Basin: Current Understanding and Future Research Directions. *Engineering*, *13*, 144–152. https://doi.org/10.1016/j.eng.2021.06.026

Mersel, M. K., Smith, L. C., Andreadis, K. M., & Durand, M. T. (2013). Estimation of river depth from remotely sensed hydraulic relationships. *Water Resources Research*, *49*(6), 3165–3179. https://doi.org/10.1002/wrcr.20176

Molle, F., Wester, P., & Hirsch, P. (2010). River basin closure: Processes, implications and responses. *Agricultural Water Management*, *97*(4), 569–577. https://doi.org/10.1016/j.agwat.2009.01.004

Munoz, S. E., Giosan, L., Therrell, M. D., Remo, J. W. F., Shen, Z., Sullivan, R. M., et al. (2018). Climatic control of Mississippi River flood hazard amplified by river engineering. *Nature*, *556*(7699), 95–98. https://doi.org/10.1038/nature26145

Nielsen, K., Stenseng, L., Andersen, O. B., Villadsen, H., & Knudsen, P. (2015). Validation of CryoSat-2 SAR mode based lake levels. *Remote Sensing of Environment*, *171*, 162–170. https://doi.org/10.1016/j.rse.2015.10.023

Pekel, J.-F., Cottam, A., Gorelick, N., & Belward, A. S. (2016). High-resolution mapping of global surface water and its long-term changes. *Nature*, 1–19. https://doi.org/10.1038/nature20584

Peterson, B. J., Holmes, R. M., McClelland, J. W., Vörösmarty, C. J., Lammers, R. B., Shiklomanov, A. I., et al. (2002). Increasing River Discharge to the Arctic Ocean. *Science*, *298*(5601), 2171–2173. https://doi.org/10.1126/science.1077445

Poff, N. L. (2019). A river that flows free connects up in 4D. *Nature*, *569*(7755), 201–202. https://doi.org/10.1038/d41586-019-01393-2

Raymond, P. A., Zappa, C. J., Butman, D., Bott, T. L., Potter, J., Mulholland, P., et al. (2012). Scaling the gas transfer velocity and hydraulic geometry in streams and small rivers. *Limnology and Oceanography: Fluids and Environments*, *2*(1), 41–53. https://doi.org/10.1215/21573689-1597669

Rocher-Ros, G., Stanley, E. H., Loken, L. C., Casson, N. J., Raymond, P. A., Liu, S., et al. (2023). Global methane emissions from rivers and streams. *Nature*, (October 2022). https://doi.org/10.1038/s41586-023-06344-6

Ruhi, A., Messager, M. L., & Olden, J. D. (2018). Tracking the pulse of the Earth's fresh waters. *Nature Sustainability*, *1*(April). https://doi.org/10.1038/s41893-018-0047-7

Saleh, F., Flipo, N., Habets, F., Ducharne, A., Oudin, L., Viennot, P., & Ledoux, E. (2011). Modeling the impact of in-stream water level fluctuations on stream-aquifer interactions at the regional scale. *Journal of Hydrology*, *400*(3–4), 490–500. https://doi.org/10.1016/j.jhydrol.2011.02.001

Schneider, R., Tarpanelli, A., Nielsen, K., Madsen, H., & Bauer-Gottwein, P. (2018). Evaluation of multi-mode CryoSat-2 altimetry data over the Po River against in situ data and a hydrodynamic model. *Advances in Water Resources*, *112*(August 2017), 17–26. https://doi.org/10.1016/j.advwatres.2017.11.027

Squillace, P. J. (1996). Observed and Simulated Movement of Bank-Storage Water. *Ground Water*, *34*(1), 121–134. https://doi.org/10.1111/j.1745-6584.1996.tb01872.x

Trautmann, T., Koirala, S., Guentner, A., Kim, H., & Jung, M. (2023). Calibrating global hydrological models with GRACE TWS: Does river storage matter? *Environmental Research Communications*. https://doi.org/10.1088/2515-7620/acece5

Trigg, M. A., Tshimanga, R. M., Ndomba, P. M., Mtalo, F., Hughes, D. A., Mushi, C. A., et al. (2022). Putting River Users at the Heart of Hydraulics and Morphology Research in the Congo Basin (pp. 541–554). https://doi.org/10.1002/9781119657002.ch28

Walsh, J. E., Bigalke, S., McAfee, S. A., Lader, R., Serreze, M. C., & Ballinger, T. J. (2023). *NOAA Arctic Report Card 2022: Precipitation*. https://doi.org/10.25923/n07s-3s69

Zakharova, E., Nielsen, K., Kamenev, G., & Kouraev, A. (2020). River discharge estimation from radar altimetry: Assessment of satellite performance, river scales and methods.

Journal of Hydrology, *583*(June 2019), 124561. https://doi.org/10.1016/j.jhydrol.2020.124561

Zhang, X., Jiang, L., Liu, Z., Kittel, C. M. M., Yao, Z., Druce, D., et al. (2023). Flow regime changes in the Lancang River, revealed by integrated modeling with multiple Earth observation datasets. *Science of The Total Environment*, *862*(December 2022), 160656. https://doi.org/10.1016/j.scitotenv.2022.160656

Zhao, Y., & Jiang, L. (2023). GRWSE-global river water surface elevation from sentinel-3 [Dataset]. Zenodo. https://doi.org/10.5281/zenodo.10060593

Zhong, R., Zhao, T., Chen, X., & Jin, H. (2022). Monitoring drought in ungauged areas using satellite altimetry: The Standardized River Stage Index. *Journal of Hydrology*, *612*(PC), 128308. https://doi.org/10.1016/j.jhydrol.2022.128308

Zomer, R., & Trabucco, A. (2022). Global Aridity Index and Potential Evapotranspiration Climate Database v3 [Dataset]. figshare. https://doi.org/10.6084/m9.figshare.20005589.v2

Zomer, R. J., Xu, J., & Trabucco, A. (2022). Version 3 of the Global Aridity Index and Potential Evapotranspiration Database. *Scientific Data*, *9*(1), 409. https://doi.org/10.1038/s41597-022-01493-1